

1 **Cathelicidin LL-37 improves bone metabolic balance in rats with**
2 **ovariectomy-induced osteoporosis via the Wnt/ β -catenin pathway**

3 Jianwei Liang¹, Jianjun Chen¹, Zhan Ye¹, Dandan Bao^{2*}

4 ¹ Department of Orthopedics, The First People's Hospital of Taizhou, Taizhou 318020,
5 China.

6 ² Department of Pharmacy, The First People's Hospital of Taizhou, Taizhou 318020,
7 China.

8

9 ***Corresponding author:**

10 Dandan Bao, Department of Pharmacy, The First People's Hospital of Taizhou, 218
11 Hengjie Road, Huangyan District, Taizhou City, Zhejiang Province, China.
12 Tel:+86-13566400505, E-mail: baodandan-007@163.com.

13

14 **Running title:** LL-37 improves bone metabolic balance in rats with osteoporosis.

15

16

17

18

19

20

21

22

23

24

25

26

27

28

29

30

31

32

33

34

35

36

37 **Summary**

38 Osteoporosis is a bone disease characterized by low bone mineral density (BMD) and
39 impaired bone microarchitecture due to the abnormal activity of osteoclasts.
40 Cathelicidins are antimicrobial peptides present in the lysosomes of macrophages and
41 polymorphonuclear leukocytes. LL-37, a cathelicidin, induces various biological
42 effects, including modulation of the immune system, angiogenesis, wound healing,
43 cancer growth, as well as inflammation, and bone loss. A previous study reported
44 direct involvement of LL-37 suppressing osteoclastogenesis in humans. Here, we
45 examined the role of LL-37 in the treatment of osteoporosis using an ovariectomy
46 (OVX) rat model. Our results showed that LL-37 significantly reduced bone loss and
47 pathological injury in OVX rats with osteoporosis. Furthermore, we found that LL-37
48 significantly increased the activity of the Wnt/ β -catenin pathway in OVX rats with
49 osteoporosis, including the increased expression of β -catenin, Osterix (Osx), and
50 Runt-related transcription factor 2 (Runx2), whereas XAV-939, an inhibitor of the
51 Wnt/ β -catenin pathway, significantly blocked the effects of LL-37 on bone loss and
52 abnormal bone metabolism. Altogether, our findings suggested that LL-37 exerted a
53 protective role in regulating bone loss and abnormal bone metabolism in rats with
54 osteoporosis by activating the Wnt/ β -catenin pathway.

55 **Keywords**

56 Cathelicidin LL-37; osteoporosis; bone metabolism; Wnt/ β -catenin pathway

57 **Introduction**

58 Osteoporosis, a systemic metabolic bone disease (BMD) characterized by
59 reduced bone mineral density, low bone mass, microarchitectural disturbance of bone
60 tissue, and increased bone fragility predisposing to fragility fractures, becomes a
61 major global health problem [1]. Osteoporosis is divided into primary osteoporosis
62 and secondary osteoporosis based on their etiology. Primary osteoporosis includes
63 postmenopausal osteoporosis (PMOP) (type I), senile osteoporosis (type II). Among
64 them, type I osteoporosis is further divided into PMOP (type IA) and male
65 osteoporosis (type IB). Osteoporosis tends to occur in people of advanced age and in
66 postmenopausal women, and patients mostly suffer from circumferential body pain
67 and fragility fractures, which are the main clinical features and seriously affect the
68 quality of life [2]. PMOP is characterized by the decreased levels of sex hormones in
69 menopause of women causing a weakened inhibitory effect on osteoclasts, resulting in
70 bone mass loss, bone microarchitectural changes, increased bone fragility, and
71 stronger bone resorption function than bone formation, causing an imbalance in bone
72 remodeling, thereby leading to decreased bone strength, has been considered as the
73 most common type of osteoporosis [3-5]. At present, clinical anti osteoporosis drugs
74 are mainly divided into two main classes, one is the bone promoting agents, such as
75 teriparatide, romosozumab; the other is bone resorption inhibitor, such as
76 bisphosphonates, estrogen, selective estrogen receptor modulators, denosumab, etc
77 [6-10]. Unfortunately, the long-term use of these drugs causes many potential side
78 effects, such as dyspepsia, constipation and so on [7, 11]. Therefore, the development
79 of safe and effective treatment strategies for osteoporosis without excessive side
80 effects is urgently required.

81 Wnt/ β -catenin signaling pathway exerts an important role in normal bone growth
82 and metabolism, such as promoting the differentiation of bone marrow mesenchymal
83 stem cells (BMSCs) into osteoblasts, stimulating the proliferation of osteoblasts,
84 inhibiting the activity of osteoclasts, and maintaining the balance between bone
85 formation and resorption [12]. It has been shown that activating Wnt/ β -catenin
86 signaling pathway can promote osteogenesis, increase bone mineral density (BMD)
87 and bone quality, improve bone structure and bone metabolism, thereby to play the
88 therapeutic role of osteoporosis[13, 14]. Therefore, the Wnt/ β -catenin signaling
89 pathway may be a potential target for the treatment of osteoporosis, and expected to

90 be used in clinical practice in the future and achieve better curative effects.

91 LL-37 is the only human member of the cathelicidin family. It is an amphipathic,
92 positively charged, 37-residue peptide generated from the precursor hCAP18 protein.
93 LL-37 is stored in the secondary granules of neutrophils, from where it is released
94 upon activation [15, 16]. It exerts activity against most gram-negative and gram-
95 positive bacteria with the primary role to exterminate the pathogens [17]. Numerous
96 studies have shown that LL-37 participates in several host immune reactions, such as
97 inflammatory responses and tissue repair, in addition to its antibacterial properties
98 [18]. LL-37 has been shown to enhance the immune response by inducing the
99 production of selective cytokines and chemokines [17]. Moreover, it is implicated in
100 several key biological processes involving non-immune cells such as angiogenesis,
101 re-epithelialization, wound closure, and the maintenance of intestinal epithelial barrier
102 integrity [19-22]. In addition, LL-37 can directly suppress osteoclastogenesis in
103 humans, thereby protecting against bone resorption induced by a bacterial infection in
104 periodontal diseases [23].

105 In the present study, we hypothesized that LL-37 regulates the bone metabolic
106 balance to attenuate ovariectomy (OVX)-induced bone loss and pathological injury in
107 ovariectomized rats. We studied bone formation and resorption, as well as the serum
108 bone metabolism parameters, and investigated the activity of the Wnt/ β -catenin
109 pathway, which could be regulated by LL-37 as reported by a previous study [24, 25].
110

111 **Materials and methods**

112 *Animals*

113 Seventy-five 3-month old female Sprague-Dawley (SD) rats weighing 230 to 240 g
114 were obtained from Chengdu Dossy Experimental Animals Co. Ltd. (certificate
115 number: SCXK [Chuang] 2019-031). All animals were maintained in an animal house
116 under controlled temperature ($23 \pm 2^\circ\text{C}$) and relative humidity (50-55%) in a 12/12 h
117 (light/dark) cycle. They were provided free access to tap water and commercially
118 available standard rat chow. Animals were allowed to acclimatize for one week before
119 the experiment. All animal experiments performed in this study were approved by the
120 Animal Ethical Committee of The First People's Hospital of Taizhou.

121

122 *OVX-induced osteoporosis and drug administration*

123 After one week of acclimatization, the rats were anesthetized and subsequently
124 subjected to bilateral OVX to establish osteoporotic animal models. As a control, the
125 rats in sham-operated (sham) group were only removed the same volume of fat tissues
126 surrounding the ovaries. One week after recovering from the surgery, OVX rats were
127 randomly divided into four groups of 15 rats each, according to their body weight and
128 named as OVX group, LL-37 treatment (OVX+LL-37) group, XAV-939 treatment
129 (OVX+XAV-939) group, and LL-37 and XAV-939 co-treatment (OVX+LL-37+
130 XAV-939) group. During the treatment, the rats in the OVX + LL-37 group were
131 intraperitoneally administrated with LL-37 (1.5 mg/kg), those in the OVX+XAV-939
132 group were intraperitoneally administrated with XAV-939 (1.0 mg/mL), those in the
133 OVX+LL-37+XAV-939 group were intraperitoneally co-administrated with LL-37
134 and XAV-939, and the rats in the OVX group and sham group were intraperitoneally
135 administrated with an equal volume of saline. The treatments were performed once
136 every 2 days. After 12 weeks of administration, the rats were anesthetized with
137 pentobarbital sodium (1%, 0.4 mL/100 g; i.p.). Next, the blood was harvested from
138 the heart, and the serum sample was stored at -80°C until biochemical analyses were
139 performed. The bilateral femurs and tibias were dissected from the animal body and
140 kept at -80°C until histological and biochemical analyses.

141

142 *Serum biochemical marker analysis*

143 The levels of serum Ca (S-Ca), and serum P (S-P) were measured by standard
144 colorimetric methods using commercially available test kits. The serum concentration
145 of tartrate-resistant acid phosphatase-5b (TRACP-5b), type I collagen C-terminal
146 telopeptide (CTX-1), bone-specific alkaline phosphatase (BALP), and procollagen
147 type I N-terminal propeptide (PINP) were determined using an appropriate
148 enzyme-linked immunosorbent assay (ELISA) kit according to the manufacturer's
149 instructions.

150

151 *Bone histomorphometry analysis*

152 The left proximal femurs (0.5 cm below the femoral head) were used to detect the
153 bone mineral density (BMD, g/cm^2), bone volume per tissue volume (BV/TV, %), the
154 thickness of trabeculae (Tb.Th, mm), number of trabeculae (Tb.N, 1/mm), and
155 separating degree of trabeculae (Tb.Sp, mm). BMD was measured using dual-energy
156 X-ray absorptiometry (DXA) (InAlyzer, Korea). BV/TV, Tb.Th, Tb.N, and Tb.Sp

157 were measured by a microcomputed tomography (micro-CT) system (SkyScan,
158 Belgium).

159

160 *Hematoxylin and eosin staining*

161 The morphology of the femur bone tissues was evaluated by hematoxylin and eosin
162 (H&E) staining under a light microscope. Briefly, tissue samples were treated with 10%
163 formaldehyde, decalcified in 15% neutral EDTA, followed by dehydration, paraffin
164 embedding, and sectioning into 5 mm-thick sections. H&E staining was performed
165 after rehydration following the protocols of Beijing Solarbio Science & Technology
166 (China). Sections were differentiated in hydrochloric acid ethanol, rinsed in water,
167 recovered in ammonia water, and then stained with eosin. Next, all samples were
168 dehydrated, rendered transparent and sealed. Histological changes were observed
169 using a light microscope. ImageJ software was used to visualize the stained trabecular
170 bone sections.

171

172 *Western blotting*

173 Rat femur bone tissue was first pulverized using liquid nitrogen and subsequently
174 immersed in the radioimmunoprecipitation (RIPA) lysis buffer (Beyotime, China)
175 containing protease inhibitor (Beyotime, China) for 15 min on ice. Following
176 centrifugation (12000 rpm, 20 min, and 4 °C), the resulting supernatants were
177 harvested, and the protein concentration was measured using the Bradford assay. Each
178 equal amount of protein sample (20 µg) was electrophoresed on a 12% SDS-PAGE
179 and transferred onto a polyvinylidene difluoride (PVDF) membrane (Millipore, USA),
180 which was afterward blocked in 5% skim milk for 2 h at room temperature.
181 Subsequently, the membrane was incubated overnight at 4 °C with the following
182 diluted primary antibodies: rat polyclonal anti-β-catenin antibody (1: 2000), rat
183 monoclonal anti-RUNX2 antibody (1: 2000), rat monoclonal anti-Osterix antibody (1:
184 2000), and rat monoclonal anti-β-actin antibody (1: 5000) (Abcam, Cambridge, UK).
185 Subsequently, blots were cultured at 25 °C for 1 h with secondary antibodies. Finally,
186 blots were visualized using an Enhanced Chemiluminescence Substrate kit (Millipore,
187 USA). The ImageJ software was used for densitometry analysis of the band intensity.

188

189 *Statistical analysis*

190 Data are expressed as the mean±standard deviation (SD) and analyzed by GraphPad

191 Prism 8.0. Comparisons between different groups were performed using the one-way
192 analysis of variance (ANOVA) with Tukey's post-hoc test. $P < 0.05$ was considered
193 statistically significant.

194

195 **Results**

196 *LL-37 improved BMD and bone microstructure in OVX rats*

197 As shown in Fig 1A–E, OVX significantly reduced the femoral BMD and impaired
198 the bone microstructure in rats, including decreased BV/TV, Tb.Th, and Tb.N and
199 increased Tb.Sp, whereas the administration of LL-37 for 12 weeks significantly
200 increased the BMD and bone microstructure strength. Interestingly, XAV-939, a
201 Wnt/ β -catenin pathway inhibitor, significantly blocked the effect of LL-37 on BMD
202 and bone microstructure in OVX rats. These results indicated that LL-37 functions to
203 maintain the bone quality in OVX rats, and the Wnt/ β -catenin pathway is an important
204 regulator of LL-37 in osteoporosis.

205

206 *LL-37 attenuated the bone loss in OVX rats*

207 We further examined the levels of serum biochemical biomarkers closely related to
208 bone metabolism and found that the levels of S-Ca and S-P remained unchanged in all
209 groups. Compared with the sham group, the bone resorption markers TRACP-5b and
210 CTx-1 and the bone formation markers PINP and BALP were significantly increased
211 in OVX group, indicated a high turnover pathology which has been always combined
212 with a net bone loss in OVX- induced osteoporosis. Twelve weeks after the LL-37
213 treatment, the changes in these biochemical biomarkers were significantly attenuated,
214 which were blocked by XAV-939 (Fig. 2A–F).

215

216 *LL-37 attenuated the pathological injury in OVX rats*

217 As shown in Fig. 3, OVX resulted in disordered and thin trabeculae, empty bone
218 lacunae, slight fractures, and considerably lower trabecular area as compared with the
219 sham group, whereas the aberrant trabecular architecture was improved by LL-37
220 treatment, which was blocked by XAV-939. These results indicated that the
221 osteoprotective effect of LL-37 was mediated by the maintenance of bone metabolism
222 homeostasis, including the increase in bone formation and a reduction in bone
223 resorption in OVX rats.

224

225 *LL-37 activated the Wnt/ β -catenin pathway in OVX rats*

226 As shown in Fig. 4, we examined the activity of the Wnt/ β -catenin pathway using
227 western blotting. We found that the expressions of β -catenin, Runx2, and Osterix were
228 significantly decreased in OVX rats, indicating that the decreased activity of
229 Wnt/ β -catenin pathway may mediate the abnormal bone turnover in OVX rats.
230 Whereas LL-37 significantly increased the expression of Wnt/ β -catenin pathway
231 when compared with the OVX group. Similarly, XAV-939 markedly blocked the
232 effect of LL-37 on the Wnt/ β -catenin pathway (Fig. 4A). These results indicated that
233 LL-37 improved bone metabolic balance and promoted normal bone turnover in rats
234 with OVX-induced osteoporosis by activating the Wnt/ β -catenin pathway.

235

236 **Discussion**

237 Osteoporosis is a metabolic bone disease and is characterized by imbalanced bone
238 formation and resorption [26, 27]. Here, we showed that OVX induced osteoporosis
239 in rats, along with pathological changes in BMD and trabecular microstructure,
240 including the increased Tb.Sp and the decreased BMD, BV/TV, Tb.Th, and Tb.N.
241 Twelve weeks after the LL-37 treatment, these changes in serum biochemical
242 parameters and BMD and trabecular structure were significantly improved. In
243 addition, the level of serum biochemical parameters, such as the bone resorption
244 markers TRACP-5b and CTx-1 and the bone formation markers PINP and BALP
245 were significantly decreased as compared with those in the OVX group after LL-37
246 treatment. These results indicated that LL-37 plays an anti-osteoporosis activity
247 through inhibition of the high bone turnover in OVX-rats.

248 Cathelicidin has a variety of unique biological functions against pathogens and
249 contributes to the induction and progression of infection, inflammation and cancer
250 [28]. LL-37 is the mature form of human cathelicidin and has been reported to
251 regulate bone homeostasis. A previous study reported that LL-37 directly suppressed
252 osteoclastogenesis in humans and acted as a protector against bone resorption induced
253 by a bacterial infection in periodontal diseases [29]. We found that LL-37
254 significantly attenuated bone loss and pathological injury by reducing overactive bone
255 turnover and maintaining serum biochemical parameter homeostasis in OVX rats.

256 The formation of osteoporosis is an extremely complicated biological process

257 involving multiple genes and factors. The Wnt/ β -catenin pathway plays a crucial role
258 in osteoporosis and significantly regulates bone formation and destruction by
259 stimulating osteoblast generation and decreasing osteoclast differentiation. In the
260 canonical Wnt/ β -catenin pathway, β -catenin accumulates in the cytoplasm and enters
261 the nucleus, where it activates the transcription of target genes and promotes bone
262 formation [30]. Previous study has shown that Wnt/ β -catenin pathway activity
263 inhibition reduces osteogenic differentiation [31, 32], whereas the activation of
264 Wnt/ β -catenin pathway accelerates osteogenic mineralization by promotion of the
265 β -catenin nuclear accumulation [1]. Thus, the factors involved in this pathway could
266 serve as potential targets of anti-osteoporosis drugs. LL-37 has been reported to
267 regulate the Wnt/ β -catenin pathway during tumorigenesis [25, 33] and differentiation
268 of adipose-derived stem cells [24]. However, whether the therapeutic role of LL-37 in
269 OVX-induced osteoporosis is exerted via Wnt/ β -catenin pathway remains unclear. We
270 found that LL-37 significantly promoted the activation of β -catenin, whereas the
271 Wnt/ β -catenin pathway inhibitor XAV-939 blocked the effect of LL-37 on β -catenin,
272 indicating that LL-37 protected against OVX-induced osteoporosis by activating the
273 Wnt/ β -catenin pathway. Meanwhile, the activated Wnt/ β -catenin may inhibit
274 overactive bone turnover and promote normal osteogenesis and osteoblast
275 differentiation by inducing the expression of Runx2 [34]. Runx2 plays a key role in
276 regulating osteoblastic function by controlling the transcription of its target genes.
277 Recent study has been reported that Runx2 induces the expression of the *COL1A1*
278 gene encoding the primary component of collagen type I by interacting with Osterix
279 [35], and plays an important role in bone homeostasis [36]. We showed that the
280 expression of Runx2 and Osterix was significantly decreased in rats with osteoporosis,
281 whereas LL-37 increased the expression of Runx2 and Osterix, which was blocked by
282 XAV-939. In addition, XAV-939 abolished the effects of LL-37 on OVX rats. These
283 results indicated that LL-37 attenuated bone loss and pathological injury by activating
284 the Wnt/ β -catenin pathway in an experimental animal model with osteoporosis.

285 In conclusion, our study revealed an important role of LL-37 in regulating
286 OVX-induced osteoporosis. The results suggested that the Wnt/ β -catenin pathway
287 primarily mediates the protective role of LL-37.

288

289 **Conflict of Interest**

290 There is no conflict of interest.

291 **Acknowledgements**

292 Not applicable

293 **Availability of data and materials**

294 All data generated or analyzed during this study are included in this published article.

295

296 **References**

- 297 1. Wang CG, Hu YH, Su SL and Zhong D. LncRNA DANCR and miR-320a
298 suppressed osteogenic differentiation in osteoporosis by directly inhibiting the
299 Wnt/beta-catenin signaling pathway. *Exp Mol Med* 2020; 52: 1310-1325.
300 10.1038/s12276-020-0475-0.
- 301 2. Jin SL, Bai YM, Zhao BY, Wang QH and Zhang HS. Silencing of miR-330-5p
302 stimulates osteogenesis in bone marrow mesenchymal stem cells and inhibits
303 bone loss in osteoporosis by activating Bgn-mediated BMP/Smad pathway. *Eur*
304 *Rev Med Pharmacol Sci* 2020; 24: 4095-4102. 10.26355/eurrev_202004_20987.
- 305 3. Black DM and Rosen CJ. Postmenopausal Osteoporosis. *N Engl J Med* 2016; 374:
306 2096-2097. 10.1056/NEJMc1602599.
- 307 4. Jackson RD and Mysiw WJ. Insights into the epidemiology of postmenopausal
308 osteoporosis: the Women's Health Initiative. *Semin Reprod Med* 2014; 32:
309 454-462. 10.1055/s-0034-1384629.
- 310 5. Zhu S, He H, Zhang C, Wang H, Gao C, Yu X and He C. Effects of pulsed
311 electromagnetic fields on postmenopausal osteoporosis. *Bioelectromagnetics*
312 2017; 38: 406-424. 10.1002/bem.22065.
- 313 6. Baron R and Hesse E. Update on bone anabolics in osteoporosis treatment:
314 rationale, current status, and perspectives. *J Clin Endocrinol Metab* 2012; 97:
315 311-325. 10.1210/jc.2011-2332.
- 316 7. Brewer L, Williams D and Moore A. Current and future treatment options in
317 osteoporosis. *Eur J Clin Pharmacol* 2011; 67: 321-331. 10.1007/s00228-011-
318 0999-2.
- 319 8. Anastasilakis AD, Polyzos SA and Makras P. Therapy of endocrine disease:
320 Denosumab vs bisphosphonates for the treatment of postmenopausal osteoporosis.
321 *Eur J Endocrinol* 2018; 179: R31-r45. 10.1530/eje-18-0056.
- 322 9. Miller PD, Pannacciulli N, Brown JP, Czerwinski E, Nedergaard BS, Bolognese

- 323 MA, Malouf J, Bone HG, Reginster JY, Singer A, Wang C, Wagman RB and
324 Cummings SR. Denosumab or zoledronic acid in postmenopausal women with
325 osteoporosis previously treated with oral bisphosphonates. *J Clin Endocrinol*
326 *Metab* 2016; 101: 3163-3170. 10.1210/jc.2016-1801.
- 327 10. Cosman F, Miller PD, Williams GC, Hattersley G, Hu MY, Valter I, Fitzpatrick
328 LA, Riis BJ, Christiansen C, Bilezikian JP and Black D. Eighteen months of
329 treatment with subcutaneous abaloparatide followed by 6 months of treatment
330 with alendronate in postmenopausal women with osteoporosis: results of the
331 ACTIVEExtend trial. *Mayo Clin Proc* 2017; 92: 200-210. 10.1016/j.mayocp.2016.
332 10.009.
- 333 11. Bolognese M, Krege JH, Utian WH, Feldman R, Broy S, Meats DL, Alam J,
334 Lakshmanan M and Omizo M. Effects of arzoxifene on bone mineral density and
335 endometrium in postmenopausal women with normal or low bone mass. *J Clin*
336 *Endocrinol Metab* 2009; 94: 2284-2289. 10.1210/jc.2008-2143.
- 337 12. Yao Q, Yu C, Zhang X, Zhang K, Guo J and Song L. Wnt/beta-catenin signaling
338 in osteoblasts regulates global energy metabolism. *Bone* 2017; 97: 175-183.
339 10.1016/j.bone.2017.01.028.
- 340 13. Shen G, Ren H, Shang Q, Zhao W, Zhang Z, Yu X, Tang K, Tang J, Yang Z,
341 Liang and Jiang X. Foxf1 knockdown promotes BMSC osteogenesis in part by
342 activating the Wnt/beta-catenin signalling pathway and prevents ovariectomy-
343 induced bone loss. *EBioMedicine* 2020; 52: 102626. 10.1016/j.ebiom.2020.
344 102626.
- 345 14. Huang Y, Xiao D, Huang S, Zhuang J, Zheng X, Chang Y and Yin D. Circular
346 RNA YAP1 attenuates osteoporosis through up-regulation of YAP1 and activation
347 of Wnt/beta-catenin pathway. *Biomed Pharmacother* 2020; 129: 110365.
348 10.1016/j.biopha.2020.110365.
- 349 15. Sørensen O, Arnljots K, Cowland JB, Bainton DF and Borregaard N. The human
350 antibacterial cathelicidin, hCAP-18, is synthesized in myelocytes and
351 metamyelocytes and localized to specific granules in neutrophils. *Blood* 1997; 90:
352 2796-2803.
- 353 16. Pahar B, Madonna S, Das A, Albanesi C and Girolomoni G. Immunomodulatory
354 Role of the Antimicrobial LL-37 Peptide in Autoimmune Diseases and Viral
355 Infections. *Vaccines (Basel)* 2020; 8: 10.3390/vaccines8030517.
- 356 17. Fabisiak A, Murawska N and Fichna J. LL-37: Cathelicidin-related antimicrobial

- 357 peptide with pleiotropic activity. *Pharmacol Rep* 2016; 68: 802-808. 10.1016/j.
358 pharep.2016.03.015.
- 359 18. Kuroda K, Okumura K, Isogai H and Isogai E. The human cathelicidin
360 antimicrobial peptide ll-37 and mimics are potential anticancer drugs. *Front*
361 *Oncol* 2015; 5: 144. 10.3389/fonc.2015.00144.
- 362 19. Koczulla R, von Degenfeld G, Kupatt C, Krötz F, Zahler S, Gloe T, Issbrücker K,
363 Unterberger P, Zaiou M, Lebherz C, Karl A, Raake P, Pfosser A, Boekstegers P,
364 Welsch U, Hiemstra PS, Vogelmeier C, Gallo RL, Clauss M and Bals R. An
365 angiogenic role for the human peptide antibiotic LL-37/hCAP-18. *J Clin Invest*
366 2003; 111: 1665-1672. 10.1172/jci17545.
- 367 20. Barlow PG, Beaumont PE, Cosseau C, Mackellar A, Wilkinson TS, Hancock RE,
368 Haslett C, Govan JR, Simpson AJ and Davidson DJ. The human cathelicidin
369 LL-37 preferentially promotes apoptosis of infected airway epithelium. *Am J*
370 *Respir Cell Mol Biol* 2010; 43: 692-702. 10.1165/rcmb.2009-0250OC.
- 371 21. Ramos R, Silva JP, Rodrigues AC, Costa R, Guardão L, Schmitt F, Soares R,
372 Vilanova M, Domingues L and Gama M. Wound healing activity of the human
373 antimicrobial peptide LL37. *Peptides* 2011; 32: 1469-1476. 10.1016/j.peptides.
374 2011.06.005.
- 375 22. Otte JM, Zdebik AE, Brand S, Chromik AM, Strauss S, Schmitz F, Steinstraesser
376 L and Schmidt WE. Effects of the cathelicidin LL-37 on intestinal epithelial
377 barrier integrity. *Regul Pept* 2009; 156: 104-117. 10.1016/j.regpep.2009.03.009.
- 378 23. Supanchart C, Thawanaphong S, Makeudom A, Bolscher JG, Nazmi K, Kornak
379 U and Krisanaprakornkit S. The antimicrobial peptide, LL-37, inhibits in vitro
380 osteoclastogenesis. *J Dent Res* 2012; 91: 1071-1077. 10.1177/0022034512
381 460402.
- 382 24. Cheng Q, Zeng K, Kang Q, Qian W, Zhang W, Gan Q and Xia W. The
383 antimicrobial peptide LL-37 promotes migration and odonto/osteogenic
384 differentiation of stem cells from the apical papilla through the Akt/Wnt/ β -catenin
385 signaling pathway. *J Endod* 2020; 46: 964-972. 10.1016/j.joen.2020.03.013.
- 386 25. Ji P, Zhou Y, Yang Y, Wu J, Zhou H, Quan W, Sun J, Yao Y, Shang A, Gu C, Zeng
387 B, Firman J, Xiao W, Bals R, Sun Z and Li D. Myeloid cell-derived LL-37
388 promotes lung cancer growth by activating Wnt/ β -catenin signaling. *Theranostics*
389 2019; 9: 2209-2223. 10.7150/thno.30726.
- 390 26. Mei F, Meng K, Gu Z, Yun Y, Zhang W, Zhang C, Zhong Q, Pan F, Shen X, Xia

- 391 G and Chen H. Arecanut (*Areca catechu* L.) seed polyphenol-ameliorated
392 osteoporosis by altering gut microbiome via LYZ and the immune system in
393 estrogen-deficient rats. *J Agric Food Chem* 2021; 69: 246-258. 10.1021/acs.jafc.
394 0c06671.
- 395 27. Behera J, Ison J, Tyagi SC and Tyagi N. The role of gut microbiota in bone
396 homeostasis. *Bone* 2020; 135: 115317. 10.1016/j.bone.2020.115317.
- 397 28. Chow JY, Li ZJ, Wu WK and Cho CH. Cathelicidin a potential therapeutic
398 peptide for gastrointestinal inflammation and cancer. *World J Gastroenterol* 2013;
399 19: 2731-2735. 10.3748/wjg.v19.i18.2731.
- 400 29. Nakamichi Y, Horibe K, Takahashi N and Udagawa N. Roles of cathelicidins in
401 inflammation and bone loss. *Odontology* 2014; 102: 137-146. 10.1007/s10266-
402 014-0167-0.
- 403 30. Liu H, Guo Y, Zhu R, Wang L, Chen B, Tian Y, Li R, Ma R, Jia Q, Zhang H, Xia
404 B, Li Y, Wang X, Zhu X, Zhang R, Brömme D, Gao S, Zhang D and Pei X.
405 *Fructus Ligustri Lucidi* preserves bone quality through induction of canonical
406 Wnt/ β -catenin signaling pathway in ovariectomized rats. *Phytother Res* 2021; 35:
407 424-441. 10.1002/ptr.6817.
- 408 31. Manolagas SC. Wnt signaling and osteoporosis. *Maturitas* 2014; 78: 233-237.
409 10.1016/j.maturitas.2014.04.013.
- 410 32. Saidak Z, Le Henaff C, Azzi S, Marty C, Da Nascimento S, Sonnet P and Marie
411 PJ. Wnt/ β -catenin signaling mediates osteoblast differentiation triggered by
412 peptide-induced $\alpha 5 \beta 1$ integrin priming in mesenchymal skeletal cells. *J Biol*
413 *Chem* 2015; 290: 6903-6912. 10.1074/jbc.M114.621219.
- 414 33. Pan XH, Quan WW, Wu JL, Xiao WD, Sun ZJ and Li D. [Antimicrobial peptide
415 LL-37 in macrophages promotes colorectal cancer growth]. *Zhonghua Zhong Liu*
416 *Za Zhi* 2018; 40: 412-417. 10.3760/cma.j.issn.0253-3766.2018.06.003.
- 417 34. Komori T. Regulation of Proliferation, Differentiation and Functions of
418 Osteoblasts by Runx2. *Int J Mol Sci* 2019; 20: 10.3390/ijms20071694.
- 419 35. Ortuño MJ, Susperregui AR, Artigas N, Rosa JL and Ventura F. Osterix induces
420 *Coll1a1* gene expression through binding to Sp1 sites in the bone enhancer and
421 proximal promoter regions. *Bone* 2013; 52: 548-556. 10.1016/j.bone.2012.
422 11.007.
- 423 36. Perez-Campo FM, Santurtun A, Garcia-Ibarbia C, Pascual MA, Valero C, Garces
424 C, Sanudo C, Zarrabeitia MT and Riancho JA. Osterix and RUNX2 are

425 transcriptional regulators of sclerostin in human bone. *Calcif Tissue Int* 2016; 99:
426 302-309. 10.1007/s00223-016-0144-4.

427

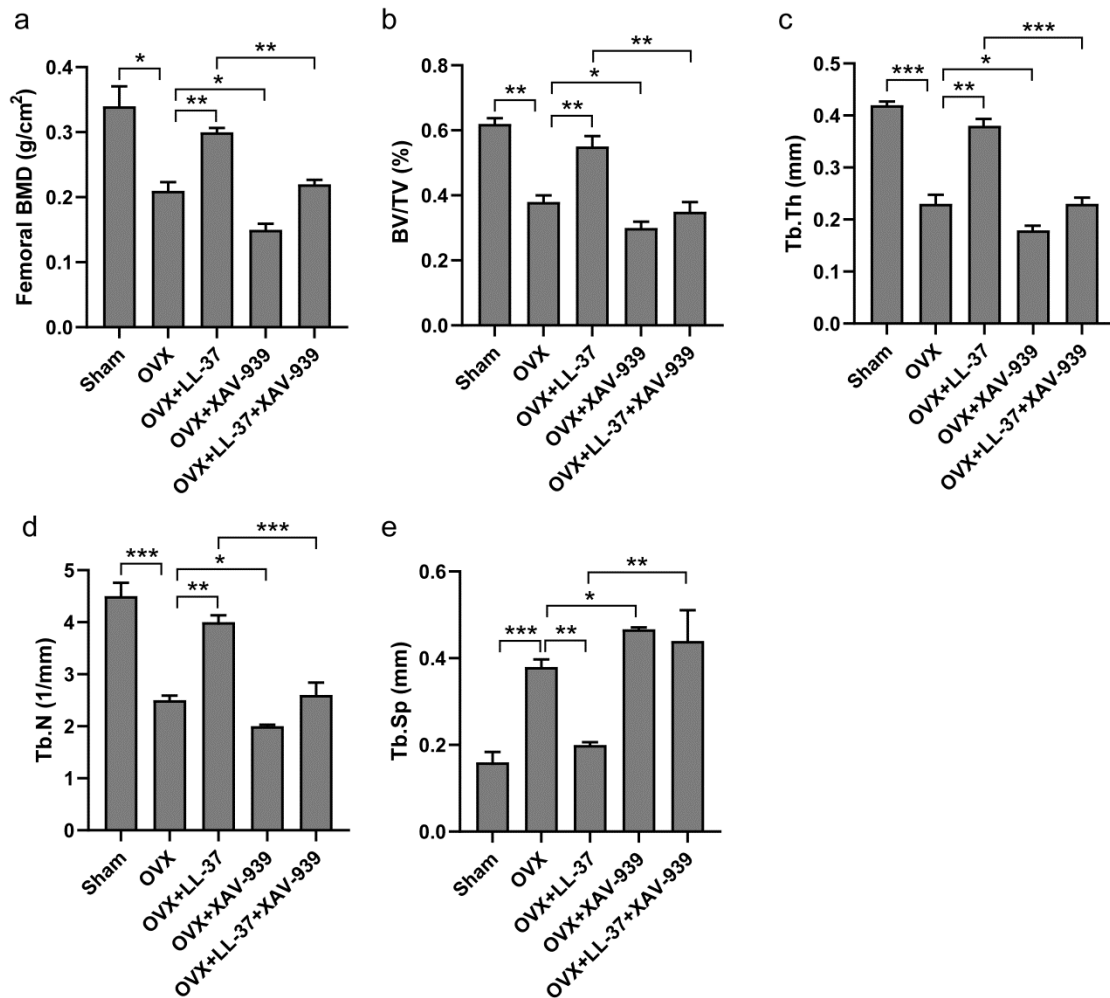
428

429

430

431

432 **Figure legends**



433

434 **Figure 1. Effect of LL-37 on BMD and bone microstructure in OVX rats.**

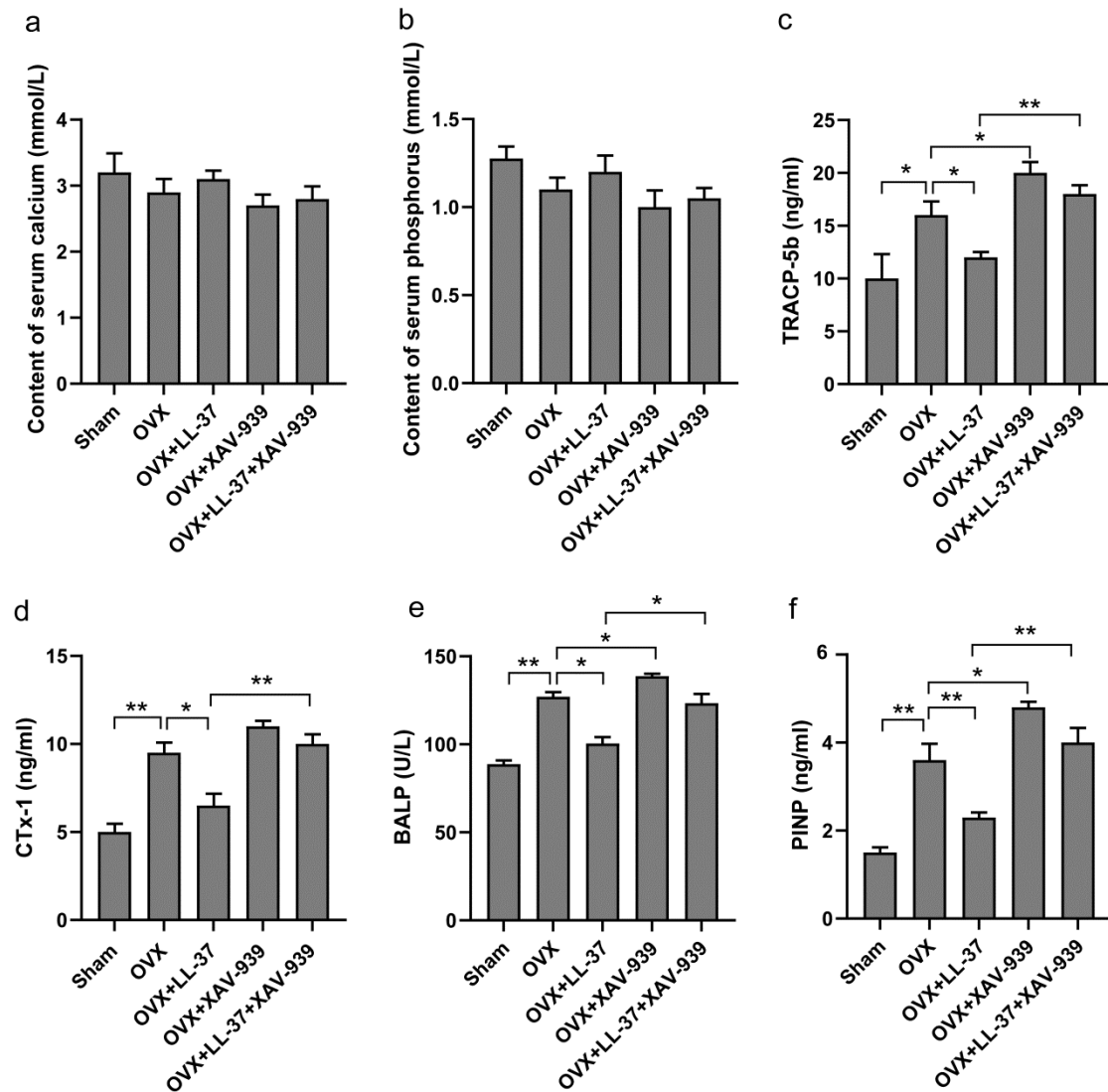
435 (a) Bone mineral density (BMD, g/cm²). (b) Bone volume/tissue volume (BV/TV, %).

436 (c) Trabecular thickness (Tb.Th, mm). (d) Trabecular number (Tb.N, 1/mm). (e)

437 Trabecular separation (Tb.Sp, mm). All bar graphs are presented as mean \pm SD. * p <

438 0.05, ** p < 0.01, *** p < 0.01.

439



440

441 **Figure 2. Effect of LL-37 on bone loss in OVX rats.**

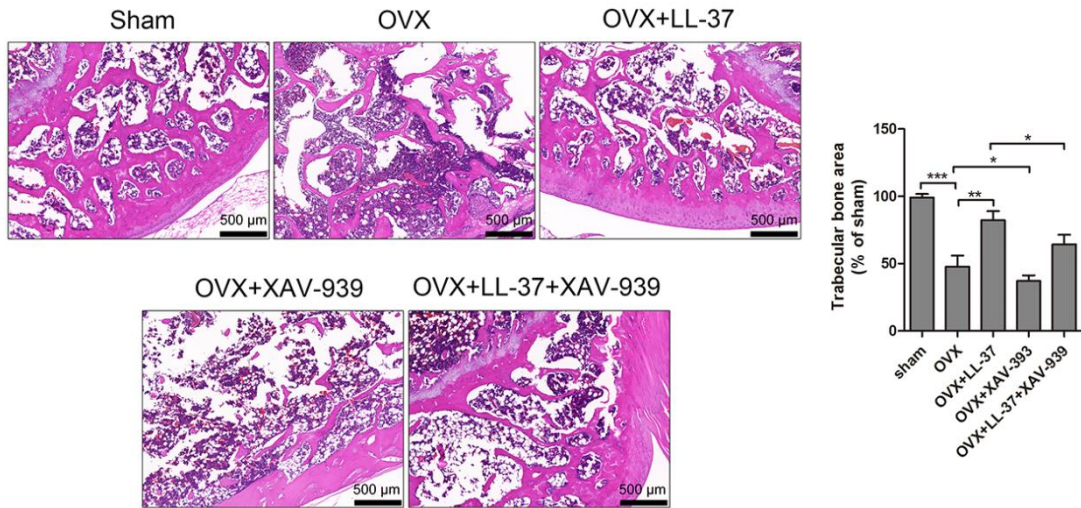
442 (a) The content of serum calcium (mmol/L). (b) The content of serum phosphorus

443 (mmol/L). (c) The level of TRACP-5b (ng/mL). (d) The level of CTx-1 (ng/mL). (e)

444 The level of BALP activity (U/L). (f) The level of PINP (ng/mL). All bar graphs are

445 presented as mean \pm SD. * $p < 0.05$, ** $p < 0.01$, *** $p < 0.01$.

446

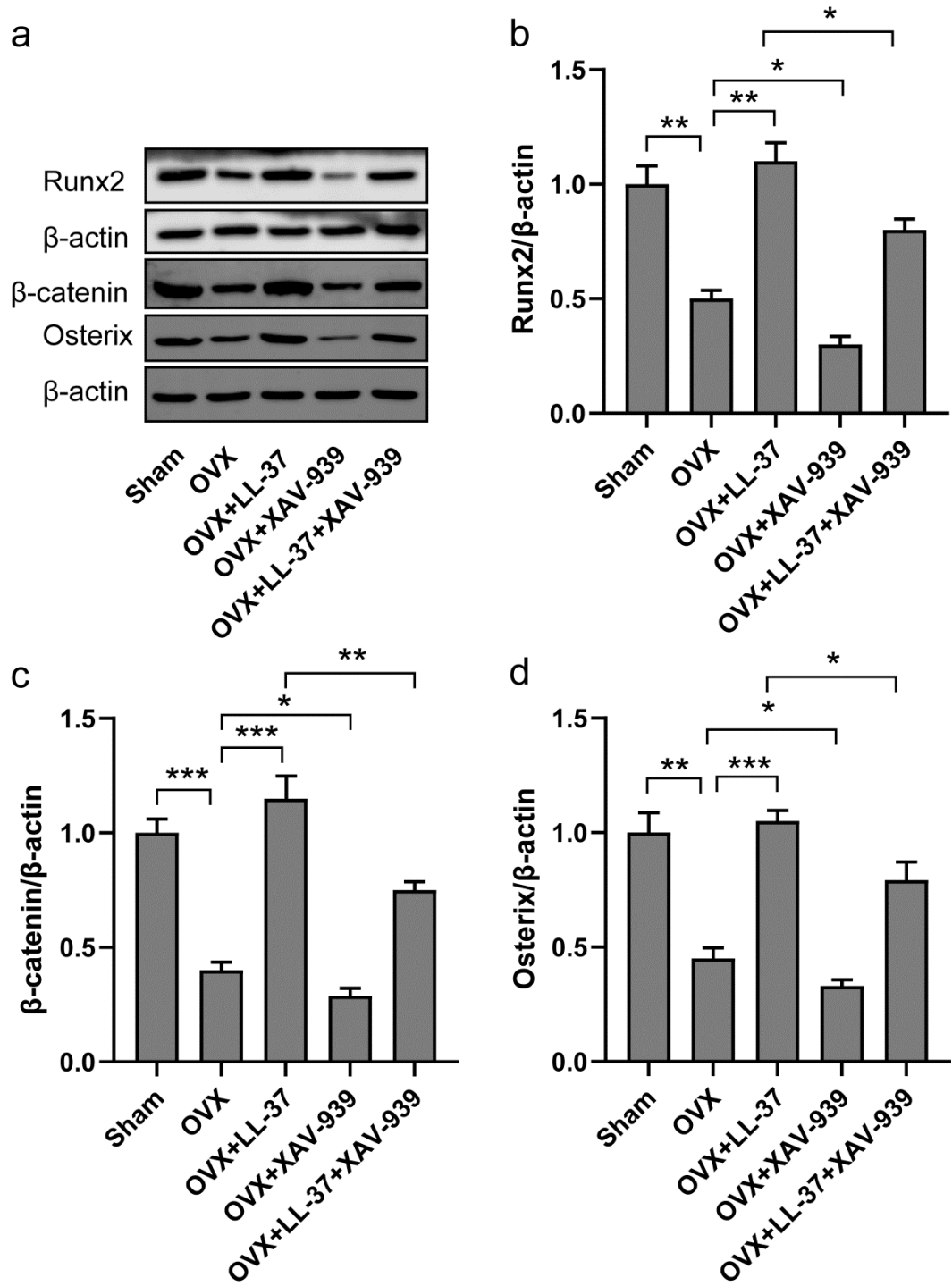


447

448 **Figure 3. Effect of LL-37 on pathological injury in OVX rats.**

449 Light microscopy of cortical and trabecular structures of the femur head (H&E
 450 staining, scale bar = 500 μ m).

451



452

453 **Figure 4. Effect of LL-37 on the activity of Wnt/β-catenin pathway in OVX rats.**

454 (a) The expression of Runx2, β-catenin, and Osterix in the femur of rats. (b)

455 Quantitative graphs of western blotting. All bar graphs are presented as mean ±SD. **p*

456 < 0.05, ***p* < 0.01, ****p* < 0.01.